Thieme

Detailed Analysis of Fetal Malformations of the Supratentorial Structures of the Brain in High-Risk Pregnancies at 12–14 Gestational Weeks by Transvaginal 3D Ultrasound Examination

Authors
Reinhard Altmann, Iris Scharnreitner, Sabine Enengl, Patrick Stelzl, Peter Oppelt, Elisabeth Reiter

Affiliations
Department of Gynaecology, Obstretrics and Gyn. Endocrinology, Kepler University Hospital, Linz, Austria

Keywords
fetal brain, first trimester screening, holoprosencephaly, migrational disorders, ganglionic eminence

received 18.01.2024
accepted after revision 10.09.2024
published online 2024

Bibliography
Ultrasound Int Open 2024; 10: a24228443
DOI 10.1055/a-2422-8443
ISSN 2509-596X

Georg Thieme Verlag KG, Rüdigerstraße 14, 70469 Stuttgart, Germany

Correspondence
Dr. Reinhard Altmann
Department of Gynaecology, Obstretrics and Gyn. Endocrinology, Kepler University Hospital
Altenberger Str. 69, 4040 Linz and
Krankenhausstrasse 9
4020 Linz
Austria
reinhard.altmann@kepleruniklinikum.at

ABSTRACT

Purpose To detect sonographic abnormalities of the supratentorial structures of the brain – future cavum septum pellucidum, cavum velum interpositum, third ventricle, ganglionic eminence and thalamus/hypothalamus – in fetuses with a crown-rump length of 45–84 mm in high-risk pregnancies.

Materials and Methods This study presents the retrospective analysis of transvaginally recorded 3D volumes of the fetal brain of 64 fetuses whose mothers consulted our ambulatory department for fetomaternal medicine for organic and/or genetic changes of their fetuses at GW 12–14. For this study we selected fetuses with 3D volume blocks of the fetal brain at best sonographic quality enabling detailed analysis and measurement of the supratentorial brain structures to correlate the results with the results of genetic analysis, ultrasound controls in later weeks of pregnancy, and fetal outcome.

Results Of 44 fetuses with genetic changes and 20 fetuses with syndromic changes, structural brain changes were found in 27 fetuses, analyzed by correlating the brain structures with the recently published structures of the brain at gestational week 12-14 in early pregnancy, presenting new details of early pathological brain development – migration disorders, milder variants of holoprosencephaly (lobar, MIH), corpus callosum agenesis, for the first time in early pregnancy.

Conclusion Supratentorial defects of the brain can be detected and analyzed in GW 12–14 in detail by direct analysis of sonopathology and visualization of pathological measurements using transvaginal 3D sonography in high quality.

Introduction

Since the introduction of first-trimester screening, increasing attention has been paid to early diagnosis of fetal structural abnormalities at weeks 12–14, in particular the fetal brain has received much attention in recent years. Complementing our two publications showing the possibilities of detailed analysis of supratentorial structures of the fetal brain – future cavum septi pellucidi (fcsp), cavum veli interpositi (cvi), third ventricle (3rdv), ganglionic eminence (GE) and thalamus/hypothalamus (Th/HyT) – in GW 12–14, this study presents the expanded possibilities for the diagnosis of pathological changes.

Materials and Methods

This was a retrospective, cross-sectional observational study including examinations between 2016 and 2023 presenting with various malformations on ultrasound and/or pathologic genetic analysis during first-trimester screening. Local ethics committee approval was obtained. Transvaginally acquired 3D volume blocks of the fetal brain of the selected fetuses were shown in excellent quality. GE ultrasound machines (E10), equipped with a transvaginal 3D probe 6–12 MHz, were used for the acquisition of the volume blocks and for the analysis of the structures. The imaging as well as the analysis of the structures were performed according to the parameters published in our previous studies on the structures of the supratentorial brain and CRL (crown-rump-length) 45 to 84 mm [1, 2]. The following were analyzed: future Cavum Septi Pellucidi antero-posterior and craniocaudal (**fCSP ap cc**), third ventricle antero-posterior, craniocaudal and lateral (**3rdv ap cc lat**), Cavum Veli Interpositi ap and cc (**CVI ap cc**), ganglionic eminence ap in an axial plane (**GE ap** – axial), the distance ganglionic eminence/insula lateral (**GE/I lat**), ganglionic eminence/basal ganglia lateral (**GE/BG lat**), ganglionic eminence/basal ganglia in a coronal plane (**GE/BG co**), thalamus/hypothalamus craniocaudal and lateral (**Th/HyT cc lat**). The above parameters were analyzed sonomorphologically and with regard to the normal values of our previous studies [1, 2]. For cvi lateral we used Loureiro's normal values published in 2012 [3]. The volume blocks stored during the initial examination were subjected to an initial analysis immediately after completion of the examination, after the confirmation of pathological brain changes a second analysis and correlation was done.

All pregnant women were offered genetic testing: fluorescence in situ hybridization and karyotyping, followed by micro array and HPO (human phenotype ontology) term based analysis if necessary. All pregnancies that were not terminated at the parents' request after abnormal genetic findings were further monitored by ultrasound until the suspected changes could be clarified.

To improve interpretability, fetuses were divided into a group of classical numerical chromosomal aberrations and a group of typical organic changes on ultrasound. The subgroups and the overlap of both groups are shown in ▶ **Table 1**. The idea of the different groups was to summarize all available cases differently to show how high the probability of brain changes was in the respective groups. All other fetuses not assigned to any of the above groups were combined in a group including various genetic and syndromic disorders with no overlap with the above groups.

Result

Group of Numerical Chromosome Aberrations

In 44 of the 64 analyzed fetuses genetic testing revealed abnormal genetic findings: nine cases of trisomy 21 (Tris 21), thirteen cases of trisomy 18 (Tris 18), five cases of trisomy 13 (Tris 13), four cases of triploidy (Tripl), nine cases of sex chromosomal aneuploidies (eight X0 and one XXX), and four fetuses presenting with various genetic disorders.

We found no dilatation of the ventricles in fetuses with isolated trisomy 21, trisomy 18, and sex chromosomal aneuploidies, supporting the observation of Manegold-Brauer that shrinking of the cho-

▶ **Table 1** Classification of numerical chromosomal aberrations in contrast to organic changes with illustration of overlap to better show correlation with supratentorial pathologies.

	a) Numerical Chromosomal Aberrations	Tris 21	Tris 18	X0/XXX	Tris 13	Tripl	b) Organic Changes		HPE	EEC	MMC
Organic findings	Total number	9	13	9	5	4	**Genetic findings**	Total number	8	3	4
	HPE				***2***	***1***		Tris 13	2		
	Cavitations	***1***						Tripl	1		
	GE, Th enlargement					***4***		Mutation CEP Gen		1	
	No additional findings	8	13	9	3			Meckel Gruber		1	
								Norm. genetics	5	1	4
	Supratent. normal	8	13	9	3	0		Supratent. normal	0	0	0
	Supratent. abnormal	***1***	0	0	***2***	***4***		***Supratent. abnormal***	***8***	***3***	***4***

roid plexus rather than dilatation of the ventricles is the relevant factor for an increased probability of trisomy 21/18/13 [4, 5]. In the trisomy 21 group, one fetus (fetus a) showed cavitations of the GE in the frontal horns. A subsequent HPO (human phenotype ontology) term-based analysis revealed two alterations in the DYNC2H1 gene of unclear clinical relevance "variants of unknown significance" (VUS) that might explain the unexpected cavitations of the GE.

In our group of five trisomy 13 fetuses we found two holoprosencephalies, described later, one fetus showed dysplasia of the fCSP and pathological narrowing of the CVI, one fetus showed no change in brain structures, a distribution consistent with the statistical probability for brain changes in trisomy 13 in the current literature [6].

Only in the triploidy group did all four fetuses show analogous changes – enlargement of the GE and Th/HyT as a uniform expression of the malformation of cortical development, representing typical expression of abnormal cell production or reduced apoptosis, consecutively accompanied by a reduction of the width of cvi and 3rd v. One fetus showed an additional absent fCSP [6].

In the heterogeneous group of diverse genetic alterations (▶ **Table 2**) – Cenani Lenz Sy, Microduplication 1q21, Noonan Syndrome, Gorlin Goltz Sy – only one fetus (fetus b) showed brain alterations – dysplasia of the fcsp according to the described morphological and metric criteria, detectable in this fetus already at weeks 12–14, was confirmed by MRI and is an occasional additional pathologic finding in Gorlin Goltz Syndrome (ORPHA:377). The brain development of all 4 fetuses was confirmed after birth.

Group of Organic Changes

Group of Encephaloceles

All three described occipital encephaloceles (EEC) showed alteration or dysplasia of the 3rd v and cvi. While one fetus (normal chromosomes) showed an occipital meningoencephalocele with an elliptic penetrating planum of 14.4 x 8.8 mm, the second fetus with a penetrating planum of 11mm revealed penetration of the meninges only (occipital meningocele). In addition, this fetus showed a mutation in the CEP gene. Fetus three in this group showed the most severe alteration with an elliptic large penetrating planum of 14 x 9 mm and additional severe dysplasia of the cerebellum and mesencephalon, genetically verified as Meckel-Gruber syndrome [7].

Group of Myelomeningoceles

All four fetuses with spina bifida (myelomeningocele - MMC) showed a reduced lateral width of the third ventricle and cvi (roof of the third ventricle) according to the study by Loureiro [3].

Holoprosencephaly Group

In the group of holoprosencephalies (HPE) we found two alobar holoprosencephalies showing a typical monoventricle and one semilobar HPE presenting with the typical fusion of the anterior horns and preserved separation of the posterior horns [8, 9].

Of particular scientific interest, however, is the diagnosis of the lesser varieties of HPE, three MIH (middle interhemispheric variant) [10, 11], and two lobar HPE in our collective where we were able to demonstrate parenchymal bridge frontal, dorsal, and parietal, respectively, as a common and typical main feature in analogy to later gestational weeks [12].

MIH variants typically present with a lack of separation of the parietal and posterior frontal lobes, an expression of the isolated fusion of these regions, while the regular separation of the polar portions of the brain is preserved. On ultrasound, an arcuate gap is the typical sign in the sagittal plane beginning anterior to the altered third ventricle, instead of the dorsal portion of the frontal lobe expected in the area and the absent fcsp extending arcuate dorsally over the thalamus above the dysplastic CVI (▶ **Fig. 1**). Complementary to the typical image of the midsagittal presentation, the axial image of the MIH variant can be used to establish the tentative diagnosis, the exact differentiation of the fusion of the individual lobes remaining reserved for the midline diagnosis.

Most difficult to diagnose in early pregnancy is lobar HPE typically defined by the absence or dysplasia of the fCSP and parenchy-

▶ **Table 2** Various syndromic and genetic disorders.

	Genetic testing		Brain development		OS	Outcome	
	Disorder	Normal	Disorder	Normal			
Cantrel Pentalogy		2	0	2	n	TOP	
Ectopia cordis		1	0	1	n	TOP	
Cenani Lenz Syndrome	1		0	1	j	TOP	
Noonan Sy	1		0	1	j	TOP	
Microd. 1q21	1		0	1	j	Birth	
Complex Malformation Sy.		2	0	2	j	TOP	
Gorlin Goltz-Sy	1		***1***		j	Birth	***fetus b***
Severe Microlissencephaly		1	***1***		n	TOP	***fetus c***
Interhemispheric Arachnoid Cyst		1	***1***		j	Birth	***fetus d***
Lissencephaly Type 2		1	***1***		j	TOP	***fetus e***
Severe Hydrops		1	***1***		j	TOP	***fetus f***

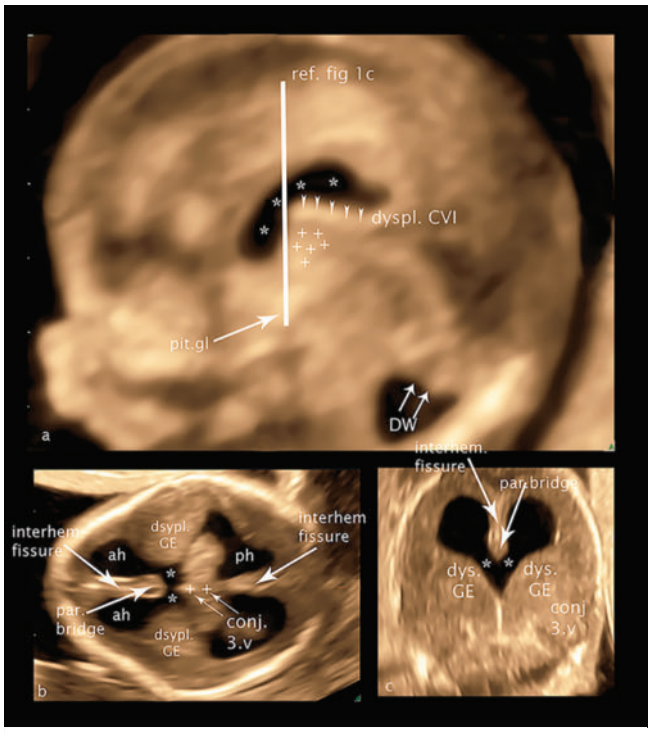

▶**Fig. 1** (HPE MIH variant): fetus 2, CRL 57 mm (**a**) midsagittal plane (**b**) axial plane (**c**) coronal plane: asterisk – typical figure showing MIH interventricular connection (parietal and posterior frontal lobes fused); plus/conj 3.v – conjoined third ventricle; (adjacent lateral walls of the 3rd v); arrowhead/dspl. CVI – dysplastic cavum veli interpositi; interhem. fissure – interhemispheric fissure; dyspl. GE – dysplastic ganglionic eminence (reduced in size, clearly shown in ▶**Fig. 1c**); par. bridge – parenchymal bridge; ah – anterior horn; ph – posterior horn; pit. gl – pituitary gland; DW - Dandy Walker Malformation, ref. ▶**Fig. 1c** – reference line showing the plane of ▶**Fig. 1c**.

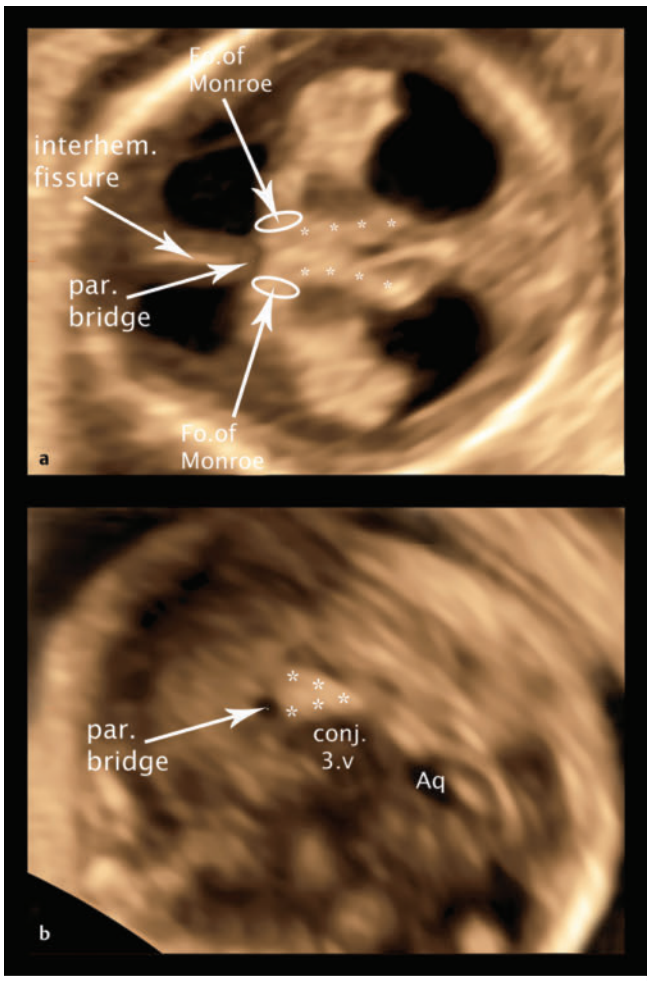

▶**Fig. 2** (lobar HPE): fetus 4, CRL 76.9 mm (**a**) axial plane (**b**) midsagittal plane: par. bridge – parenchymal bridge; interhem. fissure – interhemispheric fissure; asterisk – dyspl. choroid plexus of the third ventricle, enlarged filling cavum veli interposition; Fo. of Monroe – Foramen of Monroe; conj. 3.v – conjoined third ventricle; Aq – aqueduct

mal bridge, the only feature allowing the differentiation from the corpus callosum malformation group (▶**Fig. 2**).

The fluid gap of the 3rd ventricle is clearly narrowed or absent in our collective except for in two cases. In one of the cases (fetus 7), the 3rd ventricle dilates together with the cvi into a dorsal cyst, and in the second fetus the dilatation of the third ventricle is part of the described typical MIH change, the fusion of the ventricles, extending into the 3rd ventricle (fetus 5). Consistently valid for all cases in our collective is the absence of the fCSP. Imaging and measurements of the GE revealed a wide variation of dysplasia (hyperplasia to hypoplasia to aplasia). In contrast to the presentation of the GE, the thalamus also revealed a wide range of dysplasia without showing a clearly discernible pattern. Consequently, HPE in early pregnancy can be divided into its subgroups. Its expression as a continuum with variations analogous to the changes in the later weeks of gestation makes a clear classification difficult in some cases. Nevertheless, the differentiated analysis of the changes to be expected allows an initial clinical assessment. ▶**Table 3** shows a sonomorphological classification based on Hahn 2010 [13]. Pathological changes in the measurements are listed in ▶**Table 4**. In some cases, with pronounced hypoplastic ganglion eminence, the measurements resulted in 0 mm due to the fact that the defined measurement planes were situated above the severely dysplastic structure of the GE.

Group of Cavitations

In our collective, two fetuses were found with bilateral cavitations in the ganglionic eminence region. In fetus a the cavitations were attributed to a very rare genetic alteration, diagnosed subsequently in the course of whole exome sampling designated as VUS (see above) in addition to a free trisomy 21 previously diagnosed in the same fetus, whereas the very pronounced cavitations in fetus c were part of a complex brain malformation, which we diagnosed as microlissencephaly in perfect compliance with all changes in the description by Prefumo [14].

Group of various syndromic and genetic disorders

In the group of fetuses with various syndromic and genetic disorders without overlap to the groups presented above, **Fetus a (CRL 54 mm)** presents with cavitations described earlier. **Fetus b (CRL 60 and 83 mm) (▶Fig. 3)** showed aplasia of the fCSP at a CRL of 60 mm

▶ **Table 3** Neuroimaging features of various types of HPE in early pregnancy.

	Fetus 1	Fetus 2	Fetus 3	Fetus 4	Fetus 5	Fetus 6	Fetus 7	Fetus 8
Cortical hemisphere fusion	Frontal and parietal	Dorsal anterior/ superior	Complete	Dorsal anterior	Dorsal anterior/ super	Dorsal anterior/ superior	Dorsal anterior	Holosphere
Interhemispheric fissure and falx cerebri	Only present in a posterior location	Present in the anterior and posterior poles	Absent	Hypoplastic anterior	Hypoplastic anteriorly	Hypoplastic anteriorly and superiorly	Hypoplastic anteriorly	Absent
fcsp	Absent	Absent	Absent	Absent	Absent	Absent	Absent	Absent
Lateral ventricles	Fusion of the anterior half	Fused at their middle portion (body)	Fused	Fused superior	Fused at their middle portion (body)	Fused at their middle portion (body)	Small fusion anterior	**Monoventricle**
3rd ventricle	Almost completely adh,	Almost completely adherent, dysplastic	Almost completely adherent, dysplastic	Almost completely adherent, dysplastic	Enlarged	Almost completely adherent, dysplastic	Caudal adherent, cranial opening into dorsal cyst	Almost completely adherent, dysplastic
cvi	Extremely small	Very small	Dysplastic	Dysplastic	Enlarged	Hypoplastic	Opens into the dorsal cyst	Fused, hypoplastic
Dorsal cyst	**None**	**None**	Present	**None**	**None**	**None**	Present	**None**
Ganglionic eminence	**Asymmetric,** dysplastic, very small	Hyperplastic	Hypoplastic, dysplastic	Hypoplastic	Hypoplastic dysplastic	Hyperplastic/ dysplastic	Dysplastic/ hypoplastic	Absent
Thalamus/hypothalamus	**Normal size**	Dysplastic	Normal	Normal	Separated, enlarged due to 3.v	Dysplastic	Partially fused	Fused, hypoplastic
Parenchymal bridge	Frontal	**Superior**	**Anterior**	**Anterior**	Anterior/superior	Anterior and superior	**Anterior**	**Anterior**
Fossa post	DW variant	DW	DW	DW	Aqueductal stenosis	Normal	Normal	**Norm**
HPE type	**Semilobar**	**MIH**	**Alobar**	**Lobar**	**MIH**	**MIH**	**Lobar**	**Alobar**
Face	Facial cleft	Retrogeny	Proboscis, hypotelorism	Bilat facial cleft	Bilat facial cleft	**Normal**	Bilat facial cleft	Proboscis, hypotelorism
Genetic	Normal	Triploidy	T13	T13	normal	Normal	Normal	Normal

▲ **Table 4** Presentation of values of holoprosencephalies.

Cerebral plane		Sagittal fCSP		Sagittal 3v		Sagittal CVI		ax GE		co GE/BG	co Th/3v/VCIO			
ID	CRL	fCSPap	fCSPcc	3v ap	3v cc	CVI ap	CVI cc	GE ap	GE/I	GE/BG lat	GE/BG cc	Th lat	Th cc	3.V lat	VCI lat
fet 1	56.6	*0*	*0*	5	7.6	*0.04*	*0.05*	*0*	*0*	*0*	*0*	7	6.1	*0.06*	*0.03*
fet 2	57.0	*0*	*0*	6.2	5.2	*0.07*	*0.07*	**12.8**	**6.8**	**5.3**	**5.6**	**10.9**	7.9	*0.03*	*0.02*
fet 3	61.3	*0*	*0*	*5.4*	9.9	2.6	1.2	*0*	*0*	*0*	*0*	7.6	6.7	*0.05*	*0.07*
fet 4	76.9	*0*	*0*	6.5	6.7	2.7	2.2	5.5	3.3	*2.1*	*2*	10.5	7.6	0.7	0.8
fet 5	79.5	*0*	*0*	**10.8**	10.5	**7.5**	**3.7**	5	3.3	*2.2*	*2.8*	**12.2**	5.7	**1.9**	**1.7**
fet 6	80.4	*0*	*0*	*5.9*	9.7	*0.2*	*0.1*	*7.7*	**7.9**	**6.5**	**6.2**	**12.2**	8.7	*0*	*0*
fet 7	80.9	*0*	*0*	6.8	8.2	5.2	n. a.	*0*	*0*	*0*	*0*	9.9	6.5	**1.9**	**6.1**
fet 8	81.8	*0*	*0*	7.2	8.7	*0*	*0*	*0*	*0*	*0*	*0*	*8.8*	7.2	*0*	*0*

Measurements in correlation to the standard values taken in the published standard planes – fCSP; 3.V; CVI ap.cc GE; Th (Altmann) – CVI lat (roof of 3.V) Loureiro Measurements > 97 % bold. Measurements < 3 % light italics.

and hypoplasia of the fCSP at 83 mm. In week 26 a dysplastic corpus callosum was confirmed by MRI. Genetic diagnosis of Gorlin Goltz Sy was confirmed (▶ **Fig. 3**). **Fetus c (CRL 45.6 mm) (▶ Fig. 4)** showed huge bilateral cavitations of the ganglionic eminence, an enlarged GE, an absent fCSP, a hypoplastic thalamus, a hypoplastic 3rd v and CVI. Infratentorial the vermis showed the typical shape of a DW malformation (hypoplasia and uprotation of the vermis). Genetic testing revealed normal chromosomes including WES. Follow-up was rejected by the mother. In summary, we diagnosed microlissencephaly, also with regard to the extracranial changes in the fetus (▶ **Fig. 4**) [14]. **Fetus d (CRL 66 mm und 73 mm)** showed an absent fCSP, reduced craniocaudal length of the 3rd v, an absent CVI, a dysplastic GE, Th/HyT, and an interhemispheric arachnoid cyst. The diagnosis was confirmed in GWs 15 + 6 and 19 + 6 (details and figures published in 2022) [1]. **Fetus e (CRL 79mm)** showed hypoplasia/dysplasia of the GE and Th/HyT. The fCSP was hypoplastic, the CVI was elongated, and the cerebellar vermis and transcerebellar diameter were reduced. At GW 16 + 3, the cerebral malformations were confirmed, leading to the diagnosis of cobblestone malformation (details and figures published in 2023) [2, 15]. **Fetus f (CRL 60.1 and 83.4mm)** presented with severe hydrops. Detailed analysis of the fetal brain revealed serious enlargement of the 3rd v and cvi. The ratio between the choroid plexus and lateral ventricle diameter, between the choroid plexus and lateral ventricle length, and between the choroid plexus and lateral ventricle area were normal. Infratentorial the vermis presented hypoplastic and uprotated [16]. In contrast, the control at week 15 + 5, 16 + 6 showed normal supratentorial structures including a normal cvi and 3rd v (▶ **Fig. 5**).

All measurements of the presented fetuses are shown in ▶ **Table 5**.

The average BMI of the women was 23.01. The average length of the fetuses was 65.93 mm crown rump length.

Discussion

Ganglionic Eminence

The classification of malformation of cortical development (mcd) as enlarged (excessive proliferation or reduced apoptosis), reduced (reduced proliferation or increased apoptosis), and cavitations used by Contro 2023 [17] for pathological changes of the GE in weeks 19 to 22 is analogously applicable to our earlier collective.

Cavitation of the GE was first described by Righini in 2013 [18] on MRI. Prefumo described it on ultrasound in 2019 [14], while Brusilov described choroid plexus cysts in week 15 [19]. The two cases we found in our collective, one being part of a severe malformation of the brain (▶ **Fig. 4**), in complete analogy to Prefumo's case, was diagnosed as microlissencephaly, while the second, smaller cavitation was interpreted as a product of trisomy 21 and two alterations in the DYNC2H1 gene of unclear clinical relevance "variants of unknown significance" (VUS).

According to this classification, the enlarged MCD group included all four triploidies and one HPE, and the group of reduced MCD included eight out of nine cases of HPE. Lissencephalies, due to their very heterogeneous causality, were distributed over all 3 groups of MCD. In addition to the cases found in our collective of GE changes representing pathological cell proliferation, migration, and apopto-

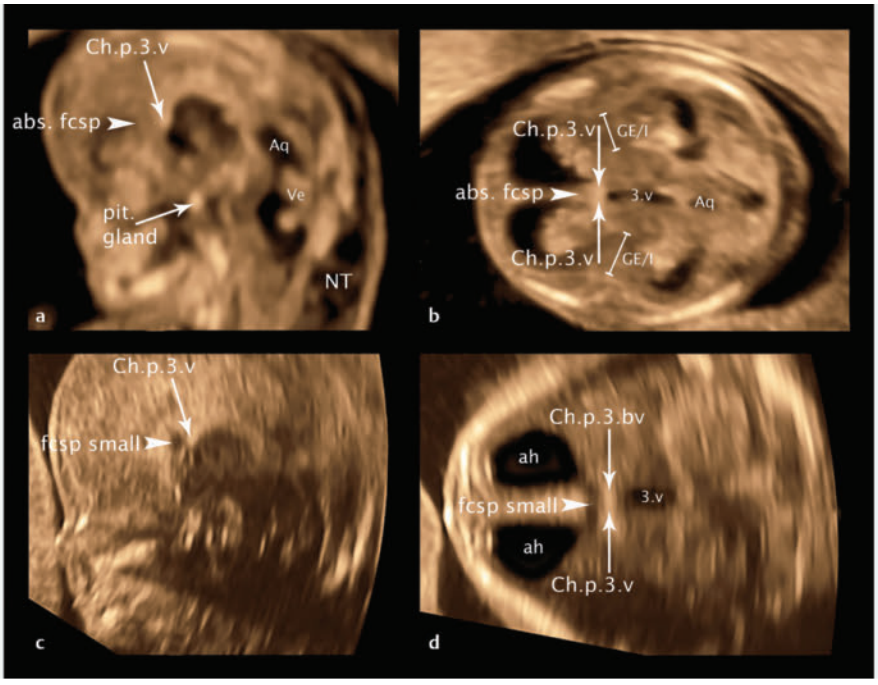

▶ **Fig. 3** (absent/hypoplastic fcsp): fetus b, CRL 60.0 mm (**a**) midsagittal plane (**b**) axial plane; CRL 83.8 mm (**a**) midsagittal plane (**b**) axial plane: abs. fcsp – absent future cavum septi pellucidi; fcsp small – future cavum septi pellucidi < 3. percentile; Ch.p.3.v – choroid plexus of the third ventricle; pit. gland – pituitary gland; Aq – aqueduct; Ve – vermis cerebelli; distance GE/I – normal distance ganglionic eminence to insula; 3.v – third ventricle; ah – anterior horn.

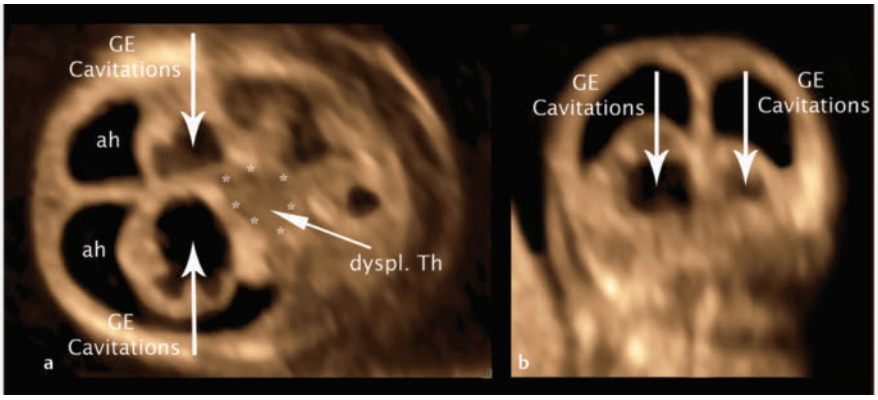

▶ **Fig. 4** (microlissencephaly): fetus c, CRL 45.6 mm (**a**) axial plane (**b**) coronal plane: GE Cavitations – cavitations of ganglionic eminence on both sides to varying degrees; asterisk/dyspl. Th – dysplastic thalamus.

sis, ischemic, destructive, or infectious processes must also be considered for differential diagnosis, even in early pregnancy.

fCSP

The use of fCSP imaging for the diagnosis of pathologies of the corpus callosum is novel as a method and is described in this study. The absence of the fCSP in all holoprosencephalies is congruent with the described changes in the later weeks of pregnancy. The absence of the fCSP in triploidy is congruent with the described literature. Unfortunately, direct evidence is missing because all pregnancies were terminated after early pregnancy.

However, three of the described isolated fCSP pathologies could be proven by investigations in the later weeks of pregnancy (fetuses b, d, and e). As a special detail, we note that the fCSP was not able to be represented at a CRL of 60 mm in one of the fetuses, whereas the fCSP showed a dysplastic reduction at a CRL of 83 mm, reflecting corpus callosum dysplasia later verified by MRI (fetus b, ▶ **Fig. 3**).

HPE

In our study we were able to show that with detailed knowledge of the anatomical structures and using transvaginal 3D examinations it is possible to diagnose lesser varieties of HPE under good examination conditions, thereby extending the most recent study by

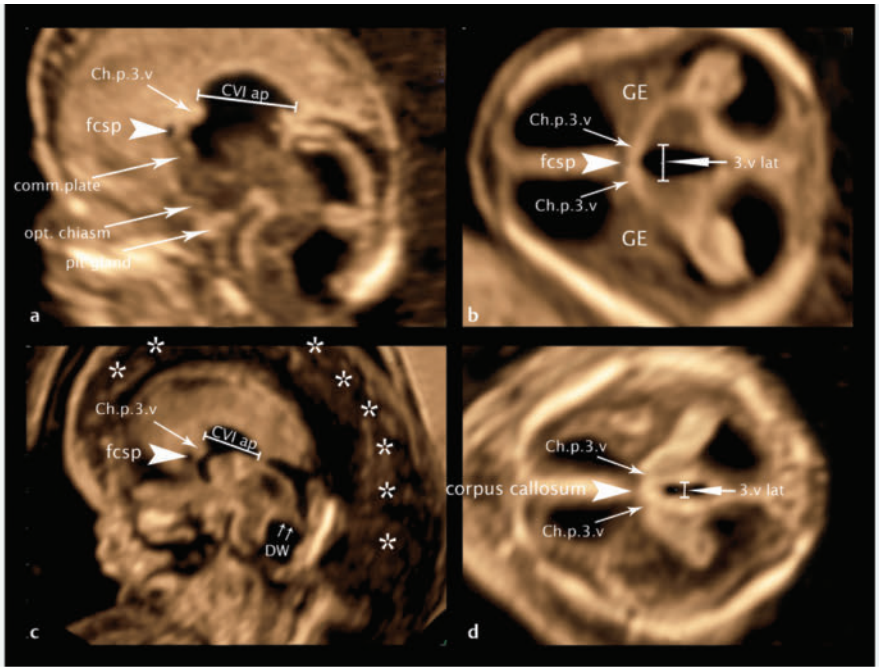

▶ **Fig. 5** (enlarged 3rd v/CVI): fetus f, CRL 60.1 mm. (**a**) midsagittal plane (**b**) axial plane; CRL 83.4 mm (**c**) midsagittal plane; GW 15 + 5 (d) axial plane: distance CVI ap – enlarged distance of cavum veli interpositi anteroposterior; distance 3.v lat – distance third ventricle lateral (enlarged in b, normal in d); arrowhead fcsp – future cavum septi pellucidi; arrowhead corpus callosum – corpus callosum; Ch.p.3.v – choroid plexus of the third ventricle; comm. plate – commissural plate; opt. chiasm – optic chiasm; pit. gland – pituitary gland; DW – Dandy Walker Malformation; asterisk – severe hydrops fetalis.

▶ **Table 5** Presentation of values of syndromes and genetic disorders.

fet a	54.0	1.3	1.3	5.9	9.1	3.2	1.5	5.2	2.3	1.4	1.3	7.0	6.2	1.1	1.1
fet b	60.0	*0*	*0*	6.5	9.6	4.5	1	6	3.3	2.7	3	8.3	7.8	0.9	0.9
	83.8	*0.9*	2.1	7.6	12.1	4.2	1.5	10.4	5	3.7	3.7	11.5	8.3	1.8	0.8
fet c	45.6	*0*	*0*	*4.3*	*5.9*	*2*	1	**7.3**	**7.7**	**7.2**	**6.5**	*4.3*	*4*	**2**	0.7
fet d	66.2	*0*	*0*	**8.7**	9	*0*	*0*	*6*	**6**	4.5	3.1	**10**	8.5	0.7	*0*
	73.0	*0*	*0*	**9.3**	11.4	*0*	*0*	*7.2*	**6.6**	**4.6**	3.2	**12.6**	7.8	1.7	*0*
fet e	78.9	*0.9*	*1.2*	7	11.2	**6.6**	2.2	*0*	*0*	*0*	*0*	**11.8**	*6.7*	**2.9**	1.3
fet f	60.1	1.2	1.2	6.5	**10.6**	**6.6**	**2**	6.4	3.8	3.0	2.8	8.2	7	**2.1**	**1.7**
	83.4	1.7	1.9	8	10.6	**8**	**3**	9.2	5.5	4.0	3.9	11	9.3	1.7	**1.5**

Measurements in correlation to the standard values taken in the published standard planes – fCSP; 3.V; CVI ap.cc GE; Th (Altmann) – CVI lat (roof of 3.V) Loureiro Measurements > 97 % bold. Measurements < 3 % light italics.

Montaguti 2022 [12] to include the possibilities of early diagnosis in weeks 12–14. For a better representation of the changes, we adapted the table prepared by Hahn 2010 [13] to point out the typical changes of the early weeks of gestation (▶ **Table 3**).

Special reference should be made to the MIH variant (fusion of the dorsal parts of the frontal and parietal lobes) and its diagnostic possibilities (▶ **Fig. 1**). The differentiation of the isolated absence of the fCSP as an expression of agenesis of the corpus callosum in the later weeks of gestation from lobar HPE, which only differs from the former with respect to the parenchymal bridge, remains to be classified as particularly difficult (▶ **Fig. 2**). The different degree of adhesion of the thalami resulting from a fusion of the medial margins of the two thalami separated in early pregnancy [20] being formed in our study period was not helpful for the differential diagnosis of the HPE variants. While alobar, semilobar holoprosencephaly and the MIH variant [21], which are already well defined in GW 12–14, are only given additional criteria by our analysis, the ultrasound images of lobar holoprosencephaly in GW 12–14, clearly following the criteria applicable in later weeks of gestation, define new diagnostic criteria where no follow-up or histological workup is available in our collective.

CVI/3rd V

The changes of the 3rd ventricle in our collective were mainly attributable to general dysplastic changes such as HPE or triploidy. Isolated changes, as described for MMC by Loureiro [3], could be reproduced, both the lateral measurements of the roof of the 3rd ventricle (now CVI) and the values of the 3rd ventricle, measured below the attachment site of the choroid plexus of the 3rd ventricle.

Furthermore, it was our intention to find out the extent to which changes in early aqueductal stenosis could influence the width of the 3rd v [22]. Analogously, we also sought to answer the question of whether an enlargement of the suprapineal recess (measurement parameter CVI ap) could be diagnostic for early aqueductal stenosis [23, 24]. Both hypotheses had to be rejected as inapplicable. Aqueductal stenosis does not dilate the 3rd ventricle nor enlarge the suprapineal recess. In contrast, we found marked enlargement of the 3rd V and CVI in one fetus, which disappeared later in pregnancy. An explanation for this finding is lacking (▶ **Fig. 5**).

Limitations: Despite all the detailed analyses described in our study, it must be emphasized that for the time being all the pathologies require further scientific analysis. Above all, however, scientific knowledge has shown in recent years that the development of brain structures can be subject to significant individual fluctuations. As a result, a clear warning should be issued against deriving decisions based on a single ultrasound diagnosis in GW 12–14. The performance of further 3D ultrasound or MRI examinations to confirm diagnoses of the developing brain should be state of the art.

Summary

Our study demonstrates that pathologic changes of the brain in weeks 12–14 (CRL 45–84 mm) can be diagnosed with precise knowledge of the anatomical conditions and with the use of appropriate high-resolution ultrasound equipment. For this reason, we recommend the presentation of suspected brain anomalies in weeks 12–14 at specialized centers.

Conflict of Interest

The authors declare that they have no conflict of interest.

References

[1] Altmann R, Scharnreitner I, Auer C et al. Visualization of the Third Ventricle, the Future Cavum Septi Pellucidi, and the Cavum Veli Interpositi at 11 + 3 to 13 + 6 Gestational Weeks on 3D Transvaginal Ultrasound Including Normative Data. Ultraschall in Med 2023; 44: e72–e82. Visualisierung des dritten Ventrikels, des zukunftigen Cavum septi pellucidi und von Cavum veli interpositi in den Schwangerschaftswochen 11 + 3 bis 13 + 6 im transvaginalen 3D-Ultraschall mit Erstellung von Normwerten. DOI: 10.1055/a-1683-6141

[2] Altmann R, Rechberger T, Altmann C et al. Development of the prosencephalic structures, ganglionic eminence, basal ganglia and thalamus at 11 + 3 to 13 + 6 gestational weeks on 3D transvaginal ultrasound including normative data. Brain Struct Funct 2023; 228: 2089–2101. DOI: 10.1007/s00429-023-02679-y

[3] Loureiro T, Ushakov F, Montenegro N, Gielchinsky Y, Nicolaides KH. Cerebral ventricular system in fetuses with open spina bifida at 11–13 weeks' gestation. Ultrasound Obstet Gynecol 2012; 39: 620–624. DOI: 10.1002/uog.11079

[4] Loureiro T, Ferreira AF, Ushakov F, Montenegro N, Nicolaides KH. Dilated fourth ventricle in fetuses with trisomy 18, trisomy 13 and triploidy at 11–13 weeks' gestation. Fetal Diagn Ther 2012; 32: 186–189. DOI: 10.1159/000338113

[5] Manegold-Brauer G, Oseledchyk A, Floeck A, Berg C, Gembruch U, Geipel A. Approach to the sonographic evaluation of fetal ventriculomegaly at 11 to 14 weeks gestation. BMC Pregnancy Childbirth 2016; 16: 3. DOI: 10.1186/s12884-016-0797-z

[6] Zalel Y, Shapiro I, Weissmann-Brenner A, Berkenstadt M, Leibovitz Z, Bronshtein M. Prenatal sonographic features of triploidy at 12–16 weeks. Prenat Diagn 2016; 36: 650–655. DOI: 10.1002/pd.4834

[7] Liao S-L, Tsai P-Y, Cheng Y-C, Chang C-H, Ko H-C, Chang F-M. Prenatal Diagnosis of Fetal Encephalocele Using Three-dimensional Ultrasound. Journal of Medical Ultrasound 2012; 20: 150–154. DOI: 10.1016/j.jmu.2012.07.005

[8] Tongsonga UT, Wanapiraka C, Chanprapapha P, Siriangkulb S. First trimester sonographic diagnosis of holoprosencephaly. International Journal of Gynecology & Obstetrics. 1999;

[9] Deeg KH, Gassner I. Sonographic diagnosis of brain malformations, part 2: holoprosencephaly – hydranencephaly – agenesis of septum pellucidum – schizencephaly – septo-optical dysplasia. Ultraschall Med 2010; 31: 548–560. quiz 561-3. DOI: 10.1055/s-0029-1245651

[10] Garrido Marquez I, Fernandez Navarro L, Moya Sanchez E. The diagnosis of the middle interhemispheric variant of holoprosencephaly with fetal MRI. Radiologia (Engl Ed) 2022; 64: 375–378. DOI: 10.1016/j.rxeng.2022.07.001

[11] Zantow E, Bryant S, Pierce SL, DuBois M, Maxted M, Porter B. Prenatal diagnosis of middle interhemispheric variant of holoprosencephaly: Report of two cases. J Clin Ultrasound 2021; 49: 765–769. DOI: 10.1002/jcu.22984

[12] Montaguti E, Cariello L, Brunelli E et al. Sonography of fetal holoprosencephaly: a guide to recognize the lesser varieties. J Matern Fetal Neonatal Med 2022; 35: 9717–9723. DOI: 10.1080/14767058.2022.2050900

[13] Hahn JS, Barnes PD. Neuroimaging advances in holoprosencephaly: Refining the spectrum of the midline malformation. Am J Med Genet C Semin Med Genet 2010; 154C: 120–132. DOI: 10.1002/ajmg.c.30238

[14] Prefumo F, Petrilli G, Palumbo G, Sartori E, Izzi C, Pinelli L. Prenatal ultrasound diagnosis of cavitation of ganglionic eminence. Ultrasound Obstet Gynecol 2019; 54: 558–560. DOI: 10.1002/uog.20236

[15] Severino M, Geraldo AF, Utz N et al. Definitions and classification of malformations of cortical development: practical guidelines. Brain 2020; 143: 2874–2894. DOI: 10.1093/brain/awaa174

[16] Volpe N, Dall'Asta A, Di Pasquo E, Frusca T, Ghi T. First-trimester fetal neurosonography: technique and diagnostic potential. Ultrasound Obstet Gynecol 2021; 57: 204–214. DOI: 10.1002/uog.23149

[17] Contro E, Volpe N, Larcher L et al. Normal and abnormal appearance of fetal ganglionic eminence on second-trimester three-dimensional ultrasound. Ultrasound Obstet Gynecol 2023; 62: 398–404. DOI: 10.1002/uog.26229

[18] Righini A, Frassoni C, Inverardi F et al. Bilateral cavitations of ganglionic eminence: a fetal MR imaging sign of halted brain development. AJNR Am J Neuroradiol 2013; 34: 1841–1845. DOI: 10.3174/ajnr.A3508

[19] Brusilov M, Malinger G, Erlik U, Haratz KK. Ganglionic eminence cavitations - these are not choroid plexus cysts!. Ultrasound Obstet Gynecol 2021; 58: 483–484. DOI: 10.1002/uog.23587

[20] Parra JED, Ripoll AP, Garcia JFV. Interthalamic adhesion in humans: a gray commissure? Anat Cell Biol 2022; 55: 109–112. DOI: 10.5115/acb.21.164

[21] Tavano I, De Catte L, De Kkeersmaecker B, Aertsen M. VP27.03: Middle interhemispheric variant of holoprosencephaly: prenatal case series and review of literature. Ultrasound in Obstetrics & Gynecology 2020; 56: 173–174. DOI: 10.1002/uog.22755

[22] Emery SP, Narayanan S, Greene S. Fetal aqueductal stenosis: Prenatal diagnosis and intervention. Prenat Diagn 2020; 40: 58–65. DOI: 10.1002/pd.5527

[23] Heaphy-Henault KJ, Guimaraes CV, Mehollin-Ray AR et al. Congenital Aqueductal Stenosis: Findings at Fetal MRI That Accurately Predict a Postnatal Diagnosis. AJNR Am J Neuroradiol 2018; 39: 942–948. DOI: 10.3174/ajnr.A5590

[24] Azzi C, Giaconia MB, Lacalm A, Massoud M, Gaucherand P, Guibaud L. Dilatation of the supra-pineal recess on prenatal imaging: early clue for obstructive ventriculomegaly downstream of the third ventricle. Prenat Diagn 2014; 34: 394–401. DOI: 10.1002/pd.4323